analytical chemistry

Letter

Cite This: Anal. Chem. XXXX, XXX, XXX−XXX

pubs.acs.org/ac

Resolution of Lipoprotein Subclasses by Charge Detection Mass Spectrometry

Corinne A. Lutomski,[†] Scott M. Gordon,[‡] Alan T. Remaley,[‡] and Martin F. Jarrold*[,†]

[†]Department of Chemistry, Indiana University, Bloomington, Indiana 47405, United States

[‡]Lipoprotein Metabolism Section, Translational Vascular Medicine Branch, National Heart, Lung, and Blood Institute, National Institutes of Health, Bethesda, Maryland 20892, United States

ABSTRACT: Lipoproteins are micelle-like assemblies that are key players in the pathogenesis of atherosclerosis. High-density lipoprotein (HDL), low-density lipoproteins (LDL), and very low density lipoprotein (VLDL) are the three major classes present in fasting plasma. Within each class, there is a broad size distribution with wide variations in protein and lipid content. The development of better metrics for cardiovascular risk is thought to depend on better characterization of lipoprotein subclasses. Using charge detection mass spectrometry (CDMS), the mass distributions of HDL, LDL, and VLDL have been directly measured for the first time. In the case of HDL, seven distinct subpopulations were resolved using a two-dimensional correlation of charge and mass. The resolved components are assigned to HDL particles containing different numbers of the key structural proteins apolipoprotein A-I and apolipoprotein A-II.

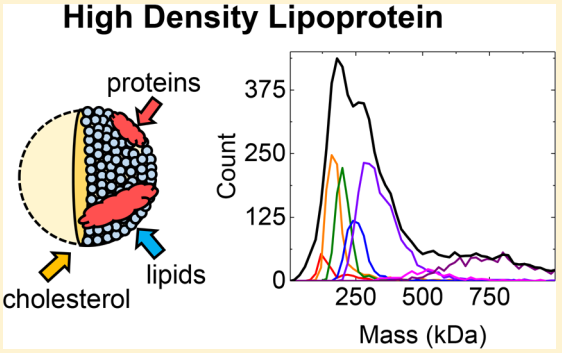

Lipoproteins consist of a core of hydrophobic triglycerides and cholesteryl esters surrounded by an amphipathic shell of phospholipid, cholesterol, and apolipoproteins. They are traditionally separated into classes by their density. Table 1 summarizes some of the properties of high-density lipoprotein (HDL), low-density lipoproteins (LDL), and very low density lipoprotein (VLDL). Lipoproteins transport lipids and cholesterol around the body and play an important role in the development of atherosclerosis and cardiovascular disease (CVD). The concentrations of HDL cholesterol and LDL cholesterol are used to predict CVD risk;[1] however, they are known to be imperfect metrics.

Table 1. Density, Diameter, and Expected Mass Ranges for HDL, LDL, and VLDL

type	density (mg/mL)	diameter (nm)	mass (MDa)
HDL	1.21−1.063	5−15	0.05−0.6
LDL	1.063−1.03	18−28	2−7
VLDL	∼1.006	30−80	8−80

Each lipoprotein density class can be further divided into several subclasses which differ in size, composition, and metabolic properties. HDL particles, in particular, have many biological effects beyond lipid transport and there is great interest in resolving and characterizing HDL subclasses.[2−4] This is a necessary first step in correlating their properties with cardiovascular disease and the development of more accurate risk metrics. The characterization of HDL is challenging because of its inherent heterogeneity. Techniques used to characterize lipoproteins include analytical ultracentrifugation, nuclear magnetic resonance, size exclusion chromatography, electrofiltration, two-dimensional electrophoretic mobility, ion mobility, liquid chromatography coupled to mass spectrometry, and related proteomics approaches.[5−13]

Charge detection mass spectrometry (CDMS)[14−22] has emerged as an important tool to characterize heterogeneous high mass species that cannot be analyzed by conventional MS. CDMS is a single particle method where the mass-to-charge ratio (m/z) and charge are directly measured for individual ions and then multiplied to obtain the mass. The masses determined for several thousand ions are then binned to give a mass spectrum. In this manuscript, we show that CDMS can resolve subclasses of HDL from a two-dimensional correlation of charge and mass.

Lipoproteins were ionized by nanoelectrospray and analyzed by a home-built charge detection mass spectrometer described elsewhere.[23−27] Ions enter the instrument through a heated capillary. They are separated from the ambient gas flow and focused into a dual hemispherical deflection energy analyzer. Energy selected ions are then focused into a modified cone trap that contains the charge detection cylinder. Potentials are placed on the front and rear end-caps of the trap, and trapped ions oscillate back and forth through the detection cylinder. Ions were trapped for 100 ms, after which the trap was opened and the trapping cycle repeated. The oscillating ion induces a periodic signal, which is amplified, digitized, and then analyzed

Received: March 13, 2018
Accepted: May 7, 2018

DOI: 10.1021/acs.analchem.8b01127
Anal. Chem. XXXX, XXX, XXX−XXX

by fast Fourier transforms. The m/z is derived from the oscillation frequency and the charge is derived from the magnitude of the fundamental and first harmonic. The m/z and charge measured for each ion are multiplied and binned to give the mass distribution.

HDL was isolated from human plasma by KBr density gradient ultracentrifugation, and human HDL, LDL, and VLDL were purchased from Academy Bio-Medical Company (Houston, TX). HDL was buffer exchanged into 5 mM ammonium bicarbonate via micro Bio-Spin columns (Bio-Rad Laboratories, Hercules, CA). LDL and VLDL were dialyzed into 15 mM and 50 mM ammonium bicarbonate, respectively.

Figure 1 show CDMS spectra for HDL (A), LDL (B), and VLDL (C) from Academy Bio-Medical. For HDL (A), the main peak is at 230 kDa and there is a shoulder at 320 kDa. A low intensity tail extends up to 4 MDa. CDMS peaks are expected to be Gaussian with a width determined by the uncertainties in the m/z and charge measurements.[28] The expected peak width for a single population at 230 kDa is ~18 kDa. The measured peak is 13 times broader. The CDMS spectrum for LDL (Figure 1B) shows two peaks: a broad distribution at 2.2 MDa and a prominent peak at 230 kDa. The low mass peak is due to an HDL impurity (see below). The peak centered on 2.2 MDa is attributed to LDL. The 2.2 MDa peak is much broader than expected for a single component (~82 kDa). The CDMS spectrum for VLDL (Figure 1C) shows a very broad mass distribution, extending from 5 to over 30 MDa. The measured masses for HDL, LDL, and VLDL fall within the expected ranges given in Table 1. Lipoproteins of all density classes are highly heterogeneous, and this accounts for the widths of the measured mass distributions.

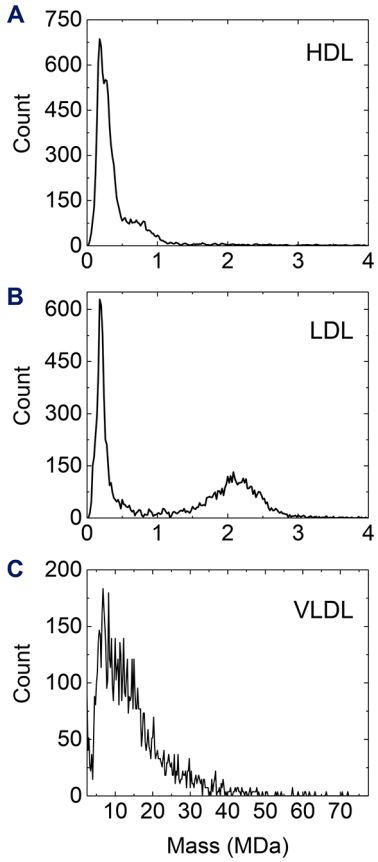

Figure 1. CDMS spectra for lipoprotein samples from Academy Biomedical: (A) HDL, (B) LDL, and (C) VLDL. The spectra were generated using 20 kDa bins for HDL and 50 kDa bins for LDL and VLDL.

The key structural protein for LDL and VLDL is apolipoprotein B100 (Apo B100). Each particle contains one Apo B100, which has a molecular weight of ~515 kDa. Thus, the peak in the spectrum for LDL (Figure 1B) at 230 kDa cannot be due to LDL. It is most likely due to HDL contamination. This was confirmed by a bottom-up proteomics experiment that revealed that the LDL sample contained some Apolipoprotein A-I, the main protein component of HDL.

The charge and mass derived from CDMS measurements are independent variables and can be correlated to obtain additional insight into the nature of the samples. Figure 2A shows a scatter plot of charge versus mass for the HDL sample in Figure 1A. Each point represents a single ion. The ions fall into "streaks" or subpopulations which have been color coded. Seven distinct subpopulations can be identified. Figure 2B shows the mass distributions for each subpopulation (using the same color code). The numbers on the figure give the average masses for each subpopulation. Figure 2C shows the subpopulations resolved in the charge versus mass scatter plot for an HDL sample prepared in house. There is good agreement between Figures 2B,C; the subpopulations identified for the commercial sample in Figure 2B are reproduced in the sample prepared in house (Figure 2C).

The "streaks" in the charge versus mass plot for HDL (Figure 2A) represent subpopulations that share similar charging properties. Streaks have been observed in other CDMS measurements of heterogeneous samples, such as micellar nanoparticles.[29] In that case, only a single streak was observed for each sample, but different streaks were observed for different compositions. This is the first time that so many streaks were resolved from a single sample. The charge increases more rapidly for the low mass streaks than for the high mass ones. This probably reflects the structure of the HDL particles with the high mass particles being closer to spherical than the low mass.

Over 50 accessory proteins and more than 200 lipid species have been identified in human HDL.[6,30−41] HDL consists of ~50% protein by mass, of which, two major structural proteins, apolipoprotein A-I (Apo A-I) and apolipoprotein A-II (Apo A-II), contribute ~70% and ~20% of the protein content, respectively.[42] The other ~10% is enzymes, lipid transfer proteins, and other minor proteins.[43] Apo A-I is conformationally flexible,[44] and particle size is related to the number and conformations of the Apo A-I proteins.[45] Some HDL subtypes carry five Apo A-I molecules per particle.[46] Because most standard analytical techniques have insufficient resolution, HDL appears to be a homogeneous mixture. However, distinct size subclasses are expected, related to both the number and conformation of Apo A-I and the number of other proteins present.[47] The differential distribution of accessory proteins across density or size-fractionated HDL has been demonstrated and supports the existence of distinct HDL subspecies.[6,48]

Given that HDL is around 50% protein and that the two major structural proteins Apo A-I (28 081 Da) and Apo A-II (17 252 Da) together contribute around 90% of the total protein then a particle with n_I Apo A-I proteins and n_{II} Apo A-II proteins would be expected to have a mass (in kDa) of around

$$m(n_I, n_{II}) = (28.081 \times n_I + 17.252 \times n_{II})/0.45 \quad (1)$$

DOI: 10.1021/acs.analchem.8b01127
Anal. Chem. XXXX, XXX, XXX−XXX

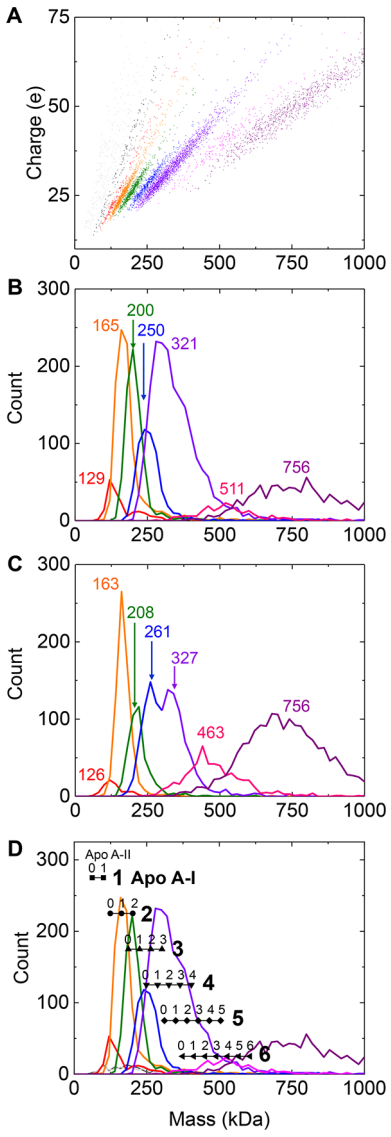

Figure 2. Resolution of HDL into subclasses. (A) Scatter plot of charge versus mass for HDL from Academy Biomedical showing color coded streaks. (B) Mass distributions of the color coded streaks in part A. The numbers give the average masses in kDa for each mass distribution. (C) Mass distributions resolved in the charge versus mass scatter plot for HDL prepared in house. 20 kDa bins were used to generate the mass distributions in parts B and C. (D) Scales giving approximate masses for HDL particles with n_I copies of Apo A-I and n_{II} copies of Apo A-II. The masses were calculated using eq 1 (see text). The large digits give the number of Apo A-I and the small digits give the number of Apo A-II. The scales overlay the mass distributions of the color-coded subpopulations for HDL from Academy Biomedical.

Masses predicted by eq 1 are shown by the scales in Figure 2D. The large digits give the number of Apo A-I proteins, with n_I ranging from 1 to 6. The smaller digits give the number of Apo A-II proteins, with n_{II} ranging from zero to $n_{II} \leq n_I$. The points on the scales give the masses from eq 1 for specific combinations of n_I and n_{II}. For example, for $n_I = 2$ and $n_{II} = 1$, the expected mass from eq 1 is 163 kDa. A distribution of masses is expected for each n_I,n_{II} combination, and the masses given by eq 1 are only approximate. However, they provide a starting point for assigning the subpopulations resolved in Figure 2. For $n_I = 2$, there are points on the scale in Figure 2D at 125, 163, and 201 kDa corresponding to $n_{II} = 0$, 1, and 2. These match up with the three lowest mass components in Figure 2B,C (which have average masses of 129/126, 165/163, and 200/208 kDa). The resolving power degrades as the mass increases so peaks due to different n_{II} are not expected to be resolved for higher masses. The resolved component centered on around 250/261 kDa in Figures 2B,C can be attributed to $n_I = 3$ and $n_{II} = 1-2$. Similarly, the peak at 321/327 kDa can be attributed to $n_I = 4$ and $n_{II} = 1-3$. Particles with $n_I = 5$ and 6 may contribute to the high mass tail on the 321−327 kDa peak and to the 511/463 kDa peak. The highest mass component in Figure 2 at 756 kDa is large for an HDL particle. A bottom-up proteomics experiment of the HDL sample revealed the presence of Apo B100, the main structural protein of LDL. Thus, an LDL impurity may be responsible for some of the high mass component observed in the HDL spectrum.

With the assignments outlined above, we attribute the components resolved in the charge versus mass scatter plot to HDL particles with different numbers of the structural proteins Apo A-I and Apo A-II. The different charging behavior probably results from changes in the shape of the particles as the number of structural proteins increases. Finally, only a small number of the possible combinations of n_I and n_{II} appear to be populated to a significant extent, or else the components would not be resolved in Figure 2.

In summary, we have shown that CDMS can measure mass distributions for HDL, LDL, and VLDL. In the case of HDL, seven subclasses can be resolved from a two-dimensional correlation of mass and charge. The resolved components can be assigned to HDL particles with different numbers of Apo A-I and Apo A-II proteins. Future analysis of lipoproteins with higher resolution CDMS should enable a more refined analysis of lipoprotein subclasses. The ultimate goal is to determine if such information can be used to develop better biomarkers for cardiovascular disease.

AUTHOR INFORMATION

Corresponding Author

*E-mail: mfj@indiana.edu.

ORCID

Martin F. Jarrold: 0000-0001-7084-176X

Notes

The authors declare no competing financial interest.

ACKNOWLEDGMENTS

This material is based on work supported by the National Science Foundation under Grant CHE-1531823.

REFERENCES

(1) Wilson, P. W. *Am. J. Cardiol.* **1990**, *66*, 7A−10A.

(2) Rosenson, R. S.; Brewer, H. B.; Chapman, M. J.; Fazio, S.; Hussain, M. M.; Kontush, A.; Krauss, R. M.; Otvos, J. D.; Remaley, A. T.; Schafer, E. J. *Clin. Chem.* **2011**, *57*, 392−410.

(3) Hafiane, A.; Genest, J. *BBA Clin.* **2015**, *3*, 175−188.

(4) Karathanasis, S. K.; Freeman, L. A.; Gordon, S. M.; Remaley, A. T. *Clin. Chem.* **2017**, *63*, 196−210.

(5) Asztalos, B. F.; Sloop, C. H.; Wong, L.; Roheim, P. S. *Biochim. Biophys. Acta, Lipids Lipid Metab.* **1993**, *1169*, 291−300.

(6) Davidson, W. S.; Silva, R. A.; Chantepie, S.; Lagor, W. R.; Chapman, M. J.; Kontush, A. *Arterioscler., Thromb., Vasc. Biol.* **2009**, *29*, 870−876.

(7) Atmeh, R. F.; Kana'an, B. M.; Massad, T. T. *Prep. Biochem. Biotechnol.* **2009**, *39*, 248−265.

DOI: 10.1021/acs.analchem.8b01127
Anal. Chem. XXXX, XXX, XXX−XXX

(8) Otvos, J. D. *Clin. Lab.* **2002**, *48*, 171−180.
(9) Jeyarajah, E. J.; Cromwell, W. C.; Otvos, J. D. *Clin. Lab. Med.* **2006**, *26*, 847−870.
(10) Nanjee, M. N.; Brinton, E. A. *Clin. Chem.* **2000**, *46*, 207−223.
(11) Caulfield, M. P.; Li, S.; Lee, G.; Blanche, P. J.; Salameh, W. A.; Benner, W. H.; Reitz, R. E.; Krauss, R. M. *Clin. Chem.* **2008**, *54*, 1307−1316.
(12) Otvos, J. D.; Rudel, L. L.; McConnell, J. P. *Clin. Chem.* **2008**, *54*, 2086−2087.
(13) Musunuru, K.; Orho-Melander, M.; Caulfield, M. P.; Li, S.; Salameh, W. A.; Reitz, R. E.; Berglund, G.; Hedblad, B.; Engström, G.; Williams, P. T.; Kathiresan, S.; Melander, O.; Krauss, R. M. *Arterioscler., Thromb., Vasc. Biol.* **2009**, *29*, 1975−1980.
(14) Shelton, H.; Hendricks, C. D.; Wuerker, R. F. *J. Appl. Phys.* **1960**, *31*, 1243−1246.
(15) Fuerstenau, S. D.; Benner, W. H. *Rapid Commun. Mass Spectrom.* **1995**, *9*, 1528−1538.
(16) Fuerstenau, S. D.; Benner, W. H.; Thomas, J. J.; Brugidou, C.; Bothner, B.; Siuzdak, G. *Angew. Chem., Int. Ed.* **2001**, *40*, 541−544.
(17) Mabbett, S. R.; Zilch, L. W.; Maze, J. T.; Smith, J. W.; Jarrold, M. F. *Anal. Chem.* **2007**, *79*, 8431−8439.
(18) Doussineau, T.; Kerleroux, M.; Dagany, X.; Clavier, C.; Barbaire, M.; Maurelli, J.; Antoine, R.; Dugourd, P. *Rapid Commun. Mass Spectrom.* **2011**, *25*, 617−623.
(19) Doussineau, T.; Désert, A.; Lambert, O.; Taveau, J.-C.; Lansalot, M.; Dugourd, P.; Bourgeat-Lami, E.; Ravaine, S.; Duguet, E.; Antoine, R. *J. Phys. Chem. C* **2015**, *119*, 10844−10849.
(20) Elliott, A. G.; Harper, C. C.; Lin, H.-W.; Susa, A. C.; Xia, Z.; Williams, E. R. *Anal. Chem.* **2017**, *89*, 7701−7708.
(21) Elliott, A. G.; Harper, C. C.; Lin, H.-W.; Williams, E. R. *Analyst* **2017**, *142*, 2760−2769.
(22) Keifer, D. Z.; Pierson, E. E.; Jarrold, M. F. *Analyst* **2017**, *142*, 1654−1671.
(23) Contino, N. C.; Jarrold, M. F. *Int. J. Mass Spectrom.* **2013**, *345*−*347*, 153−159.
(24) Contino, N. C.; Pierson, E. E.; Keifer, D. Z.; Jarrold, M. F. *J. Am. Soc. Mass Spectrom.* **2013**, *24*, 101−108.
(25) Pierson, E. E.; Keifer, D. Z.; Contino, N. C.; Jarrold, M. F. *Int. J. Mass Spectrom.* **2013**, *337*, 50−56.
(26) Pierson, E. E.; Contino, N. C.; Keifer, D. Z.; Jarrold, M. F. *J. Am. Soc. Mass Spectrom.* **2015**, *26*, 1213−1220.
(27) Keifer, D. Z.; Shinholt, D. L.; Jarrold, M. F. *Anal. Chem.* **2015**, *87*, 10330−10337.
(28) Pierson, E. E.; Keifer, D. Z.; Asokan, A.; Jarrold, M. F. *Anal. Chem.* **2016**, *88*, 6718−6725.
(29) Doussineau, T.; Santacreu, M.; Antoine, R.; Dugourd, P.; Zhang, W.; Chaduc, I.; Lansalot, M.; D'Agosto, F.; Charleux, B. *ChemPhysChem* **2013**, *14*, 603−609.
(30) Heinecke, J. W. *J. Lipid Res.* **2009**, *50*, S167−S171.
(31) Davidsson, P.; Hulthe, J.; Fagerberg, B.; Camejo, G. *Arterioscler., Thromb., Vasc. Biol.* **2010**, *30*, 156−163.
(32) Hoofnagle, A. N.; Heinecke, J. W. *J. Lipid Res.* **2009**, *50*, 1967−1975.
(33) Heller, M.; Stalder, D.; Schlappritzi, E.; Hayn, G.; Matter, U.; Haeberli, A. *Proteomics* **2005**, *5*, 2619−2630.
(34) Hortin, G. L.; Shen, R. F.; Martin, B. M.; Remaley, A. T. *Biochem. Biophys. Res. Commun.* **2006**, *340*, 909−915.
(35) Karlsson, H.; Leanderson, P.; Tagesson, C.; Lindahl, M. *Proteomics* **2005**, *5*, 1431−1445.
(36) Rezaee, F.; Casetta, B.; Levels, J. H.; Speijer, D.; Meijers, J. C. *Proteomics* **2006**, *6*, 721−730.
(37) Kunitake, S. T.; Carilli, C. T.; Lau, K.; Protter, A. A.; Naya-Vigne, J.; Kane, J. P. *Biochemistry* **1994**, *33*, 1988−1993.
(38) Skipski, V. P.; Barclay, M.; Barclay, R. K.; Fetzer, V. A.; Good, J. J.; Archibald, F. M. *Biochem. J.* **1967**, *104*, 340−352.
(39) Wiesner, P.; Leidl, K.; Boettcher, A.; Schmitz, G.; Liebisch, G. *J. Lipid Res.* **2009**, *50*, 574−585.
(40) Yetukuri, L.; Soderlund, S.; Koivuniemi, A.; Seppanen-Laakso, T.; Niemela, P. S.; Hyvonen, M.; Taskinen, M. R.; Vattulainen, I.; Jauhiainen, M.; Oresic, M. *J. Lipid Res.* **2010**, *51*, 2341−2351.
(41) Quehenberger, O.; Armando, A. M.; Brown, A. H.; Milne, S. B.; Myers, D. S.; Merrill, A. H.; Bandyopadhyay, S.; Jones, K. N.; Kelly, S.; Shaner, R. L.; Sullards, C. M.; Wang, E.; Murphy, R. C.; Barkley, R. M.; Leiker, T. J.; Raetz, C. R.; Guan, Z.; Laird, G. M.; Six, D. A.; Russell, D. W.; McDonald, J. G.; Subramaniam, S.; Fahy, E.; Dennis, E. A. *J. Lipid Res.* **2010**, *51*, 3299−3305.
(42) Jayaraman, S.; Gantz, D. L.; Gursky, O. *Biochemistry* **2006**, *45*, 4620−4628.
(43) Kontush, A.; Chapman, M. J. *High-Density Lipoproteins: Structure, Metabolism, Function, and Therapeutics*; Wiley: Hoboken, NJ, 2011.
(44) Davidson, W. S.; Thompson, T. B. *J. Biol. Chem.* **2007**, *282*, 22249−22253.
(45) Curtiss, L. K.; Bonnet, D. J.; Rye, K. A. *Biochemistry* **2000**, *39*, 5712−5721.
(46) Massey, J. B.; Pownall, H. J.; Macha, S.; Morris, J.; Tubb, M. R.; Silva, R. A. G. D. *J. Lipid Res.* **2009**, *50*, 1229−1236.
(47) Huang, R.; Silva, R. A. G. D.; Jerome, W. G.; Kontush, A.; Chapman, M. J.; Curtiss, L. K.; Hodges, T. J.; Davidson, W. S. *Nat. Struct. Mol. Biol.* **2011**, *18*, 416−422.
(48) Gordon, S. M.; Deng, J. Y.; Lu, L. J.; Davidson, W. S. *J. Prot. Res.* **2010**, *9*, 5239−5249.

DOI: 10.1021/acs.analchem.8b01127
Anal. Chem. XXXX, XXX, XXX−XXX